Research Article | Vol. 25, No. 16 | 7 Aug 2017 | OPTICS EXPRESS 19603
Optics EXPRESS

Cladding-like waveguide fabricated by cooperation of ultrafast laser writing and ion irradiation: characterization and laser generation

JINMAN LV,[1] ZHEN SHANG,[1] YANG TAN,[1,*] JAVIER RODRÍGUEZ VÁZQUEZ DE ALDANA,[2] AND FENG CHEN[1]

[1]*School of Physics, State Key Laboratory of Crystal Materials, Shandong University, Jinan 250100, China*
[2]*Departamento Física Aplicada, Facultad Ciencias, Universidad de Salamanca, Salamanca 37008, Spain*
[*]*tanyang@sdu.edu.cn*

Abstract: We report the surface cladding-like waveguide fabricated by the cooperation of the ultrafast laser writing and the ion irradiation. The ultrafast laser writes tracks near the surface of the Nd:YAG crystal, constructing a semi-circle columnar structure with a decreased refractive index of – 0.00208. Then, the Nd:YAG crystal is irradiated by the Carbon ion beam, forming an enhanced-well in the semi-circle columnar with an increased refractive index of + 0.0024. Tracks and the enhanced-well consisted a surface cladding-like waveguide. Utilizing this cladding-like waveguide as the gain medium for the waveguide lasing, optimized characterizations were observed compared with the monolayer waveguide. This work demonstrates the refractive index of the Nd:YAG crystal can be well tailored by the cooperation of the ultrafast laser writing and the ion irradiation, which provides an convenient way to fabricate the complex and multilayered photonics devices.

© 2017 Optical Society of America

OCIS codes: (230.7390) Waveguides, planar; (140.0140) Lasers and laser optics; (160.5690) Rare-earth-doped materials.

References and links

1. L. Dong, L. Reekie, and J. L. Cruz, "Long period gratings formed in depressed cladding fibers," Electron. Lett. **33**(22), 1897–1898 (1997).
2. Z. Shang, Y. Tan, S. Akhmadaliev, S. Zhou, and F. Chen, "Cladding-like waveguide structure in Nd:YAG crystal fabricated by multiple ion irradiation for enhanced waveguide lasing," Opt. Express **23**(21), 27612–27617 (2015).
3. D. Monzon-Hernandez, A. N. Starodumov, A. Goitia, V. N. Filippov, V. P. Minkovich, and P. Gavrilovic, "Stress distribution and birefringence measurement in double-clad fiber," Opt. Commun. **170**(4–6), 241–246 (1999).
4. J. C. Knight, T. A. Birks, P. S. Russell, and D. M. Atkin, "All-silica single-mode optical fiber with photonic crystal cladding," Opt. Lett. **21**(19), 1547–1549 (1996).
5. X. Xin, N. Zhong, Q. Liao, Y. Cen, R. Wu, and Z. Wang, "High-sensitivity four-layer polymer fiber-optic evanescent wave sensor," Biosens. Bioelectron. **91**, 623–628 (2017).
6. C. Grivas, "Optically pumped planar waveguide lasers, Part I: Fundamentals and fabrication techniques," Prog. Quantum Electron. **35**(6), 159–239 (2011).
7. H. X. Kang, H. T. Zhang, and D. S. Wang, "Thermal-induced refractive-index planar waveguide laser," Appl. Phys. Lett. **95**(18), 181102 (2009).
8. R. Villagomez, R. Lopez, R. Cortes, and V. Coello, "Integral plug-in RF module in a CO_2 hybrid-waveguide laser: Its performance and overall evaluation," Optik (Stuttg.) **118**(3), 110–114 (2007).
9. W. Loh, F. J. O'Donnell, J. J. Plant, M. A. Brattain, L. J. Missaggia, and P. W. Juodawlkis, "Packaged, High-Power, Narrow-Linewidth Slab-Coupled Optical Waveguide External Cavity Laser (SCOWECL)," IEEE Photonic Tech. Lett. **23**(14), 974–976 (2011).
10. E. A. Avrutin, B. S. Ryvkin, J. T. Kostamovaara, and D. V. Kuksenkov, "Strongly asymmetric waveguide laser diodes for high brightness picosecond optical pulses generation by gain switching at GHz repetition rates," Semicond. Sci. Technol. **30**(5), 055006 (2015).

#300554 https://doi.org/10.1364/OE.25.019603
Journal © 2017 Received 21 Jun 2017; revised 26 Jul 2017; accepted 29 Jul 2017; published 4 Aug 2017

Optics EXPRESS

11. L. Ge, J. Lin, J. Li, H. Y. Qu, J. T. Wang, J. Liu, J. W. Dai, Z. W. Zhou, B. L. Liu, H. M. Kou, and Y. Shi, "Densification behavior, doping profile and planar waveguide laser performance of the tape casting YAG/Nd:YAG/YAG ceramics," Opt. Mater. **60**, 221–229 (2016).
12. F. Qiu and T. Narusawa, "Refractive index change mechanisms in swift-heavy-ion-implanted Nd:YAG waveguide," Appl. Phys. B-laser O. **105**(4), 871–875 (2011).
13. M. Khanlary, D. E. Hole, and P. D. Townsend, "Ion beam luminescence of Nd:YAG," Nucl. Instrum. Meth. B. **227**(3), 379–384 (2005).
14. F. Chen and J. R. Vázquez de Aldana, "Optical waveguides in crystalline dielectric materials produced by femtosecond-laser micromachining," Laser Photonics Rev. **8**(2), 251–275 (2014).
15. T. Calmano, J. Siebenmorgen, O. Hellmig, K. Petermann, and G. Huber, "Nd:YAG waveguide laserwith 1.3 W output power, fabricated by direct femtosecond laser writing," Appl. Phys. B-Lasers O. **100**(1), 131–135 (2010).
16. T. Calmano and S. Mueller, "Crystalline Waveguide Lasers in the Visible and Near-Infrared Spectral Range," IEEE J. Top. Quant. **21**(1), 1602213 (2015).
17. N. D. Psaila, R. R. Thomson, H. T. Bookey, N. Chiodo, S. Shen, R. Osellame, G. Cerullo, A. Jha, and A. K. Kar, "Er:Yb-doped oxyfluoride silicate glass waveguide laser fabricated using ultrafast laser inscription," IEEE Photonic. Techl. Lett. **20**(1–4), 126–128 (2008).
18. I. Chartier, B. Ferrand, D. Pelenc, S. J. Field, D. C. Hanna, A. C. Large, D. P. Shepherd, and A. C. Tropper, "Growth and low-threshold laser oscillation of an epitaxially grown Nd:YAG waveguide," Opt. Lett. **17**(11), 810–812 (1992).
19. F. Qiu and T. Narusawa, "Refractive index change mechanisms in swift-heavy-ion-implanted Nd:YAG waveguide," Appl. Phys. B-Lasers O. **105**(4), 871–875 (2011).
20. J. R. Macdonald, S. J. Beecher, P. A. Berry, G. Brown, K. L. Schepler, and A. K. Kar, "Efficient mid-infrared Cr:ZnSe channel waveguide laser operating at 2486 nm," Opt. Lett. **38**(13), 2194–2196 (2013).
21. T. Calmano, A.-G. Paschke, J. Siebenmorgen, S. T. Fredrich-Thornton, H. Yagi, K. Petermann, and G. Huber, "Characterization of an Yb:YAG ceramic waveguide laser, fabricated by the direct femtosecond-laser writing technique," Appl. Phys. B **103**(1), 1–4 (2011).
22. G. Corrielli, A. Seri, M. Mazzera, R. Osellame, and H. de Riedmatten, "Integrated Optical Memory Based on Laser-Written Waveguides," Phys. Rev. Appl. **5**(5), 054013 (2016).
23. C. Cheng, H. L. Liu, Z. Shang, W. J. Nie, Y. Tan, B. R. Rabes, J. R. Vázquez de Aldana, D. Jaque, and F. Chen, "Femtosecond laser written waveguides with MoS_2 as satuable absorber for passively Q-switched lasing," Opt. Mater. Express **6**(2), 367 (2016).
24. Y. C. Jia, Y. Tan, C. Cheng, J. R. Vázquez de Aldana, and F. Chen, "Efficient lasing in continuous wave and grapheme Q-switched regimes from Nd:YAG ridge waveguides produced by combination of swift heavy ion irradiation and femtosecond laser ablation," Opt. Express **22**(11), 2900–2908 (2014).
25. L. Wang, F. Chen, X. L. Wang, K. M. Wang, Y. Jiao, L. L. Wang, X. S. Li, Q. M. Lu, H. J. Ma, and R. Nie, "Low-loss planar and stripe waveguides in Nd^{3+}-doped silicate glass produced by oxygen-ion implantation," J. Appl. Phys. **101**(5), 053112 (2007).
26. H. L. Liu, J. R. Vázquez de Aldana, B. del Rosal Rabes, and F. Chen, "Waveguiding microstructures in Nd:YAG with cladding and inner dual-line configuration produced by femtosecond laser inscription," Opt. Mater. **39**, 125–129 (2015).
27. Y. Tan, C. Zhang, F. Chen, F. Q. Liu, D. Jaque, and Q. M. Lu, "Room-temperature continuous wave laser oscillations in Nd:YAGceramic waveguides produced by carbon ion implantation," Appl. Phys. B-lasers O. **103**(4), 837–840 (2011).
28. RSoft Design Group, Computer software BandSLOVE, *http://www.rsoftdesign.com*
29. Y. Tan, L. Ma, Z. Gao, M. Chen, and F. Chen, "Two-Dimensional heterostructure as a platform for surface-enhanced Raman scattering," Nano Lett. **17**(4), 2621–2626 (2017).
30. Y. Tan, X. B. Liu, Z. L. He, Y. R. Liu, M. W. Zhao, H. Zhang, and F. Chen, "Tuning of Interlayer Coupling in Large-Area Graphene/WSe2 van der Waals Heterostructure via Ion Irradiation: Optical Evidences and Photonic Applications," ACS Photonics **4**(6), 1531–1538 (2017).
31. L. Ma, Y. Tan, M. Ghorbani-Asl, R. Boettger, S. Kretschmer, S. Zhou, Z. Huang, A. V. Krasheninnikov, and F. Chen, "Tailoring the optical properties of atomically-thin WS_2 via ion irradiation," Nanoscale, doi:10.1039/C7NR02025B.
32. Y. Tan, R. Y. He, J. Macdonald, A. K. Kar, and F. Chen, "Q-switched Nd:YAG channel waveguide laser through evanescent field interaction with surface coated grapheme," Appl. Phys. Lett. **105**(10), 101111 (2014).

1. Introduction

The cladding waveguide/fiber is an optical structure with triple layers, which have a gradient refractive index increasing from the outer to the core, so called the outer cladding, inner cladding and core. Compared with the monolayer waveguide/fiber, the cladding structure allows a higher coupling efficiency with the diode laser, and most of guided light is concentrated in the core leading to higher energy intensity. In a laser system, the laser oscillation can be optimized by the cladding-like structure, such as a lower threshold and higher slope efficiency [1–5].

Optics EXPRESS

The waveguide laser is a micro laser system with the waveguide as the resonant cavity and the gain medium, which is one basic active component for integrated photonic circuits [6–10]. The choice of the optical material and the design of the structure for the waveguide are both important for efficiency laser emission. The neodymium doped yttrium aluminum garnet sproved to be one of the mostly used gain media for waveguide lasers. Until now, efforts to fabricate waveguide lasers in Nd:YAG laser crystal have predominantly focused on ion beam implantation/irradiation [11–13], ultrafast laser writing [14–17] and epitaxial growth technique [18]. Among them, the ion irradiation and ultrafast laser writing are recognized as the most powerful techniques. The ion irradiation increases the refractive index of the YAG crystal, and constructs an enhanced-well for optical waveguide construction [19]. While, the ultrafast laser writing makes tracks inside the YAG crystal with the decreased refractive index, and the waveguide core is typically surrounded by a number of tracks (Type II and Type III configuration waveguides). The ion irradiation is extensively applied for the planar waveguide fabrication. And the ultrafast laser writing is a powerful and promising method to fabricate optical waveguides with diverse geometries [20–22].

In this work, we applied ultrafast laser writing and ion irradiation to fabricate a surface cladding waveguide structure in Nd:YAG crystal, composed by an outer cladding layer (fs-laser induced damage tracks), an inner cladding (the region between tracks and ion irradiated region) and a core layer (the region irradiated by Carbon ion). Due to the multilayer structure, the Nd:YAG cladding waveguide has a higher coupling efficiency with the pump laser. And the guided light is much easier coupled into the core from the outer cladding, leading to a higher optical intensity. As a result, the laser oscillation in the Nd:YAG cladding waveguide has a higher slope efficiency and a lower laser threshold. Additionally, due to the high output power and ensuring spatial mode control, this work proves a new way to develop double-cladding, cladding-pumped or large-mode-area planar waveguides. Furthermore, the tungsten disulfide nanoplatelets were added onto the surface of the Nd:YAG cladding waveguide as the saturable absorber through the evanescent field interaction. Under the 810 nm laser pumping, the Q-switched pulses were observed at the wavelength of 1064 nm.

2. Experimental in details

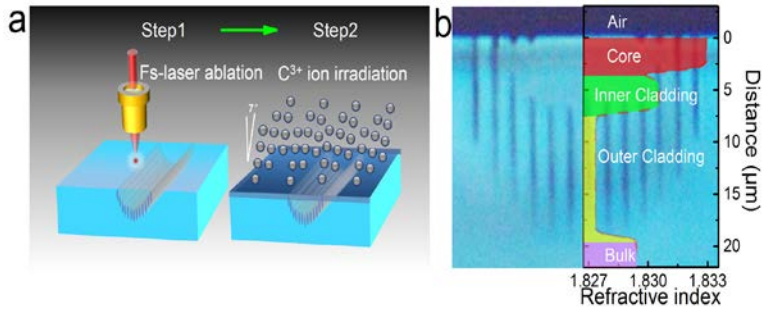

Fig. 1. (a) The schematic process of ultrafast laser writing (Step1) and ion irradiation (Step2) for the cladding-like waveguide. (b) The microscope image of the sample cross section and corresponding refractive index as a function with the depth of the distance from the sample surface.

The Nd:YAG crystal (doped by 1 at.% Nd^{3+} ions) used in this work was cut into dimensions of 10 × 9 × 2 mm^3 with biggest facets optically polished. The cladding-like waveguide was fabricated on the biggest surface of the Nd:YAG wafer following steps in Fig. 1(a). First, tracks were written by fs-laser near the surface of Nd:YAG crystal and constructed a semi-circle columnar structure. An amplified Ti:Sapphire laser system (Spitfire, Spectra Physics) was applied for generating linearly polarized 120 fs pulses at a central wavelength of 800 nm (with 1 kHz repetition rate and 1 mJ maximum pulse energy). The writing velocity was 500 μm/s with a 3-μm separation between adjacent two tracks. Details of the laser-writing

Optics EXPRESS

Nd:YAG waveguide has been reported in [23]. Then, to obtain cladding-like waveguide, C^{3+} ions at energy of 6 MeV and fluence of 3×10^{14} ions/cm^2 were irradiated on top of the biggest surface (i.e., the depressed cladding waveguide surface) to form a planar waveguide layer at Peking University. Details of the ion-irradiating Nd:YAG waveguide has been reported in [24]. As a consequence, a cladding-like waveguide with a thickness of 3.8 μm was constructed on the Nd:YAG crystal near the surface. Afterward, to improve the waveguides performance, we employed thermal annealing treatment at 220 °C for 4 h in open air. A microscope (Axio Imager, Carl Zeiss) was utilized to image the cross sections of the cladding-like waveguide in Nd:YAG crystal.

The waveguide laser operation experiments in CW and pulsed regimes were both performed by using end pumping system at room temperature. A polarized light beam at a wavelength of 810 nm from a tunable CW Ti:Sapphire laser (Coherent MBR 110) was coupled into the waveguide by a spherical convex lens with focus length of 25 mm. The Fabry–Perot laser cavity was formed by the two polished end facets without additional dielectric mirrors. To generate the laser pulses, a WS_2 film as the saturable absorber was dispersed into a solution and spin-coated onto the surface of the waveguide. The generated waveguide lasers were collected by utilizing a 20 × microscope objective lens (N.A. = 0.4) and imaged by an IR CCD. We used a spectrometer with resolution of 0.2 nm to analyze the emission spectra of the CW laser beam from the waveguide, and an oscilloscope (Tektronix TDS 202 2B, 200 MHz) to analyze the pulse trains of the pulsed waveguide laser beams. The propagation loss of the waveguide was measured to be 0.6 dB/cm following the method in [25].

3. Results and discussion

3.1 Characterizations

Figure 1(b) shows the microscopic image of the cross section of the waveguide, which has a cladder-like distribution. The outer cladding was a semi-circle columnar surrounded by tracks with a diameter of 20 μm. The inner cladding was between the irradiated and ultrafast laser written regions. And the core was formed by the Carbon ion irradiation with a thickness of 3.8 μm. We reconstructed the refractive index profile of the waveguide by the intensity profile fitting method (IPFM) [2] which was assumed to be superposed by Carbon ion irradiation and Ultrafast laser writing following the expression below:

$$\Delta n(z) = a\,\Delta n_1(z) + b\,\Delta n_2(z) \tag{1}$$

where Δn is the refractive index change; Δn_1 [26] and Δn_2 [27] are the refractive index change induced by fs-laser writing and Carbon ion irradiation, respectively.

The inset in Fig. 1(b) displays the reconstructed refractive index profile with the red dashed line (a = 1 and b = 1). As one can see, the refractive index in the outer cladding is decreased with $\Delta n = -0.00208$, which forms an optical barrier and confines the light between tracks and the surface of Nd:YAG crystal. The refractive index of the inner cladding was slightly increased due to the compression effect induced by the ultrafast laser writing process. And the core has the maximum refractive index change of $\Delta n = + 0.00112$. Based on reconstructed refractive index, the guided mode of the cladding waveguide was calculated by the Finite Difference Beam Propagation Method (FD-BPM) [28]. As shown in Figs. 2(a) and 2(b), the cladding guided light supports single modes at the wavelength of 1064 nm with the polarization of light vertical [Fig. 2(a), *s*-polarization) / parallel (Fig. 2(b), *p*-polarization] to the surface of the waveguide. We also measured guided modes with the detecting light at the wavelength of 1064 nm shown in Fig. 2(c) and Fig. 2(d). Compared with measured and calculated results, one can conclude that the simulated results match quite well with the experimental data.

Optics EXPRESS

In order to demonstrate optimizations of the cladding-like waveguide, guided modes of waveguides fabricated by a single technology (Ultrafast laser writing or Carbon ion irradiation) were also calculated by FD-BPM. Compared with the monolayer waveguide fabricated by ultrafast laser writing [as shown in Fig. 2(e) or Fig. 2(f)], the guided light is confined in the core, resulting in much higher optical intensities. Additionally, compared with the monolayer waveguide by Carbon ion irradiation [as shown in Fig. 2(g) or Fig. 2(h)], the cladding-like waveguide is the channel waveguide instead of the planar waveguide. Besides the coupling efficiency of the cladding-like waveguide has raised with respect to the monolayer waveguide by Carbon ion irradiation based on the stimulation. Further can be much easily coupled into the core due to the confinement of the inner and outer cladding. The superiority of the cladding-like waveguide is the balance of the high coupling efficiency and the high intensity of the light, which gives us a hint for the design of the novel waveguide laser with enhanced laser properties.

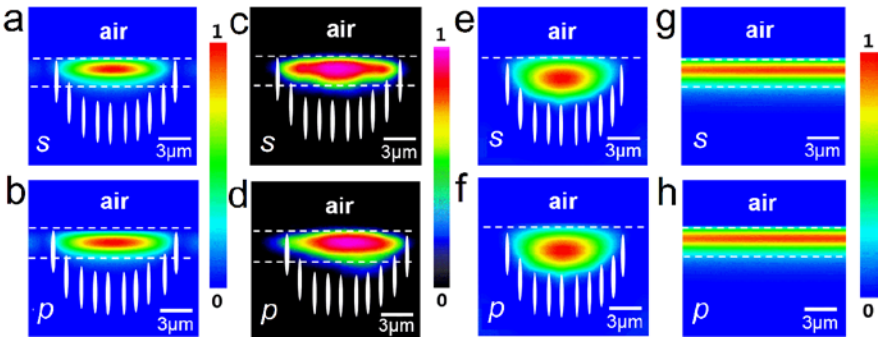

Fig. 2. Simulated near-field intensity distribution of the cladding-like waveguide at 1064nm along *s*-polarization (a) and *p*-polarization (b). Measured near-field intensity distribution of the cladding-like waveguide at 1064nm along *s*-polarization (c) and *p*-polarization (d). Simulated near-field intensity distribution of the monolayer waveguide by ultrafast laser writing along *s*-polarization (e) and *p*-polarization (f) and by Carbon ion irradiation along *s*-polarization (g) and *p*-polarization (h).

3.2 Applications

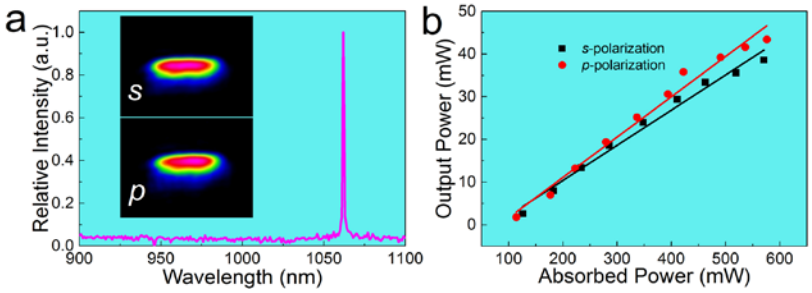

Fig. 3. (a) Laser emission spectrum from the Nd:YAG cladding-like waveguide. The inset graphs display the laser mode of the laser from the waveguide cores at both *s*- and *p*-polarization at the lasing wavelength of ~1064 nm. (b) The CW waveguide laser output powers at 1064 nm as a function of the absorbed light power at 808 nm. The dark rectangular and red rounded symbols stand for the data along *s*- and *p*- polarization, respectively. The solid lines represent the linear fit of the experimental data.

The cladding-like waveguide was used as the gain medium and resonant cavity for the CW laser oscillation. Figure 3(a) depicts laser emission spectrum of the output light from the cladding-like Nd:YAG waveguide The central wavelength of the output laser is at 1064 nm with a Full-Width Half-Maximum (FWHM) of ~0.4 nm, corresponding to the fluorescence of $^4F_{3/2} \rightarrow {}^4I_{11/2}$ transmission in the Nd^{3+} ions. The insets of Fig. 3(a) show the intensity

Optics EXPRESS

distributions of the laser modes at both *s* and *p* polarizations, exhibiting single mode profiles. Figure 3(b) shows the output power of the CW laser as a function of the pump power, with the pumping laser along *s* and *p* polarizations. Based on the linear fitting of the measured data, it is determined the lasing thresholds for 1064 nm oscillations are 24.4 mW, and the slope efficiencies are 24.2% (*s* - polarization) and 27.8% (*p* - polarization), respectively.

In order to obtain the pulsed laser, WS_2 nanoplatelets were dispersed into a solution and spin-coated onto the surface of the cladding-like waveguide, as the saturable absorber (Fig. 4(a) [29–31]. The morphology of the WS_2 nanoplatelets is determined by TEM (Transmission Electron Microscope) in Figs. 4(b) and 4(c). Above the lasing threshold, the stable pulse train was observed due to the modulation of the WS2 nanoplatelets as shown in Fig. 4(d). The repetition rate increased with increasing pump power, which is quite in good agreement with the previous work [32]. Figure 4(e) illustrates the powers of the output laser as a function of the power of the pumping laser at 810 nm along the *s*-polarization. The lasing threshold was 120 mW, which is slightly higher than CW laser. However, it is lower than the Q-switched laser in [24]. Figure 4(f) shows the dependence of the repetition rate and pulse duration along with the pumping power at *s*-polarized. As one can see, efficient short–pulse waveguide lasers with repetition rate in scale of MHz with the help of the evanescent–field interaction between the waveguide laser and WS_2. As Fig. 4(f) depicted, with the pumping power increasing, the pulse repetition rates were monotonous increasing from 1.6 MHz to 4.6 MHz, resulting in tunable ranges of 3 MHz. Meanwhile the pulse widths became smooth and the minimum pulse widths were obtained to be 45 ns.

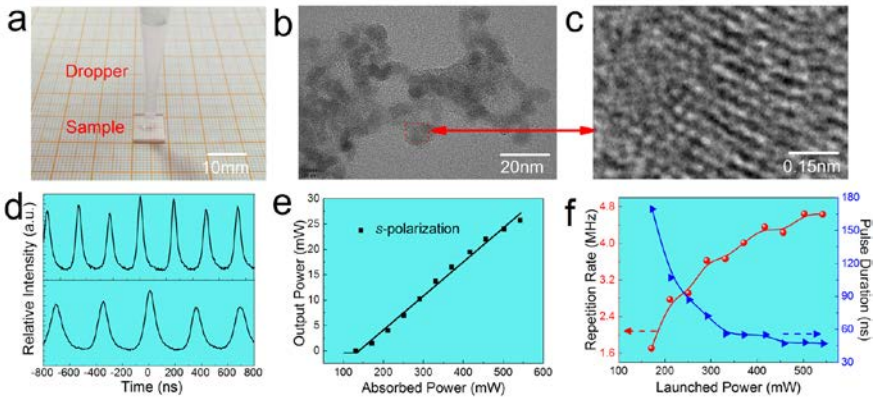

Fig. 4. (a) The image of coating WS_2, (b) low magnification TEM image, and (c) high magnification TEM image. (d) The exhibition of pulse trains at *s*-polarized input power of 152mW (up), at 84mW (down). (e) The power of the output laser as a function of pump power, and (f) the repetition rate and the pulse duration of the pulsed laser

4. Conclusion

We fabricated the surface cladding-like waveguide by the cooperation of the ultrafast laser writing and the ion irradiation. This cladding-like waveguide was proved to have higher intensity density compared to the monolayer waveguide, which is convenient for the laser oscillation. Under the pump at 810 nm, the stable CW and the Q-switched waveguide lasing at 1064 nm were realized. The stable CW waveguide laser has a maximum output power of 28.4 mW and the slope efficiency of 27.8%. Using the WS_2 as the saturable absorber, the Q-switched pulsed laser was achieved with pulse duration of 45 ns. This work suggests that the technique with cooperation of the ultrafast laser writing and the ion irradiation may be an efficient method to fabricate diverse waveguides in a large range of optical materials.

Funding

National Natural Science Foundation of China (No.11535008).

212.128.135.19 {ts '2021-05-19 05:13:13'}